BMC Pulmonary Medicine

RESEARCH

Open Access

Evaluation of respiratory muscle dysfunction in patients with idiopathic pulmonary fibrosis: a prospective observational study with magnetic resonance imaging

Xiaoyan Yang[1,2†], Hongyi Wang[2,3†], Anqi Liu[3,4], Yifei Ni[3,4], Jianping Wang[4,5], Yueyin Han[2,3], Bingbing Xie[2], Jing Geng[2], Yanhong Ren[2], Rongguo Zhang[6], Min Liu[4,5*] and Huaping Dai[2,3,7*]

Abstract

Objective Respiratory muscle dysfunction in patients with idiopathic pulmonary fibrosis (IPF) is a big challenge for treatment and rehabilitation. To quantitatively assess diaphragm and chest wall dysfunction using dynamic Magnetic Resonance Imaging (Dyn-MRI) in patients with IPF.

Methods Ninety-six patients with IPF and 50 gender- and age-matched controls were prospectively included and underwent D-MRI with a dynamic fast spoiled gradient-recalled echo sequence. Respiratory muscles function were assessed with thoracic anterior-posterior (AP), left-right (LR), cranial-caudal (CC) metrics. Moreover, lung area ratios, height (DH), and area (DA) of diaphragm curvature between end-inspiration and end-expiration during both quiet and deep breathing.

Results During quiet breathing, the functional metrics of the diaphragm and chest wall were comparable between IPF patients and controls. However, during deep breathing, IPF patients exhibited significantly reduced ratios of AP, CC, and lung area compared to controls. Moreover, the median ratios of DH and DA were higher in IPF patients than in controls (DH: 0.96 vs. 0.81, $p < 0.001$; DA: 1.00 vs. 0.90, $p < 0.001$). Furthermore, the ratios of AP, CC, and lung area during deep breathing were found to correlate with pulmonary function, total lung volume, and 6-minute walk distance.

Conclusion D-MRI demonstrated dysfunction in the diaphragm and chest wall among IPF patients, with respiratory muscle dysfunction showing a correlation with the severity of disease.

Trial registration This article presents a prospective observational study that does not include the outcomes of any healthcare interventions on human participants. The study was registered on September 11, 2018, under the registration number NCT03666234.

†Xiaoyan Yang and Hongyi Wang contributed equally to this work.

*Correspondence:
Min Liu
mikie0763@126.com
Huaping Dai
daihuaping@ccmu.edu.cn

Full list of author information is available at the end of the article

Keywords Idiopathic pulmonary fibrosis, Magnetic resonance imaging, Diaphragm, Chest wall

Introduction

Idiopathic pulmonary fibrosis (IPF) is a chronic and progressive disorder with an estimated median survival time of 3–5 years after diagnosis [1]. Patients with IPF are characterized by restrictive ventilatory dysfunction, progressively deteriorated exercise tolerance, impaired health-related quality of life (HRQoL), and poorer survival [1]. Evaluation of respiratory muscle function is helpful for the treatment and nursing of patients with deteriorated dyspnea and exercise intolerance [2].

Conventional pulmonary function tests (PFTs) can indirectly indicate mobility of the respiratory muscles; however, it is impossible to quantitatively visualize the chest wall and diaphragmatic motion. Recent studies with CT and diaphragmatic ultrasound indicated that the decrease in skeletal muscle mass and strength was associated with increased mortality and a worse prognosis in interstitial lung disease (ILD) patients [3–6]. With diaphragmatic ultrasound, fibrosis ILD (FILD) patients were shown to have decreased diaphragmatic mobility during deep breathing which is associated with reduced lung volumes [7]. However, both CT and ultrasound possess have inherent limitations. CT is associated with exposure to ionizing radiation and 4D-CT with significant image artifacts, which may affect the shape representation of normal anatomy. In addition, ultrasound lacks the capability to synchronously measure the chest wall and diaphragmatic motion.

Magnetic resonance imaging (MRI) allows for non-ionizing radiation and enables simultaneous visualization of the diaphragmatic and chest wall motion during the respiratory cycle. Yang et al. assessed the diaphragmatic and chest wall motion in healthy population [8]. Several studies evaluated diaphragmatic motion with Dynamic-MRI (Dyn-MRI) in patients with idiopathic scoliosis and neuromuscular diseases [9–12]. The structure and motion of the diaphragm and chest wall also have been applied to assess healthy people and some chronic respiratory diseases, such as chronic obstructive pulmonary disease (COPD) and asthma [13–15]. However, diaphragmatic and chest wall motion in IPF patients and the correlation of respiratory muscle dysfunction and the severity of IPF have not been reported.

Therefore, we aimed to assess the diaphragmatic and chest wall function in IPF patients during quiet and deep breathing using D-MRI, and to explore the relationship between the diaphragmatic and chest wall motion with and severity indicators of IPF including dyspnea, PFTs, HRQoL, exercise tolerance, and the extent of pulmonary fibrosis observed on high- resolution CT (HRCT).

Methods

Study cohort and design

This single-center prospective observational study was approved by our Institutional Ethics Committee (2019-123-K85-1). All participants provided written informed consent. From August 2020 to April 2022, patients with IPF and gender-and age-matched healthy controls were prospectively enrolled. IPF was diagnosed by the multidisciplinary consensus based on the international standard of 2011 ATS/ERS/JRS/ALAT criteria [1]. All patients underwent HRCT, PFTs, a 6-minute walk distance test (6MWD), and chest MRI within 48 h. Figure 1 is the flowchart detailing how participants were selected and how the research was conducted. Patients with other lung diseases, such as malignancy, acute infection, neuromuscular disease, a history of chest or abdominal surgery, or renal dysfunction were excluded. Subjects who had MRI contraindications or failed to undergo MRI or PFTs were also excluded. Gender and age-matched people with normal HRCT and PFTs were included as the control group. They also underwent HRCT, PFTs, 6MWD, and chest MRI within 48 h.

For assessment of the severity of IPF patients, in addition to PFTs, HRCT, and 6MWD, dyspnea was quantified by the Medical Research Council (MRC) scale [16]. Dyspnea was classified as mild (MRC = 1), moderate (MRC = 2 or 3), and severe (MRC = 4 or 5). HRQoL was quantified using the St. George's Respiratory Questionnaire (SGRQ) [17], a respiratory-specific Questionnaire including respiratory symptoms, activity, and psychosocial impact of the disease [17]. Higher scores (ranging from 0 to 100) correspond to worse quality of life.

Pulmonary function test

All participants underwent PFTs according to the standards of ATS/ERS [18]. PFT measurements included the percentage of predicted forced vital capacity (FVC%), percentage of forced expiratory volume in one second (FEV1%), FEV1/FVC%, percentage of predicted total lung capacity (TLC%), and percentage of predicted DLco corrected for measured hemoglobin (DLco%).

High-resolution CT

All participants underwent HRCT using multidetector CT systems (Toshiba Aquilion ONE TSX-301 C/320; Philips iCT/256). The whole chest was craniocaudally scanned in the supine position from the lung apex to the lowest hemidiaphragm in deep breathing. Acquisition parameters and reconstruction parameters were by CT standards: tube voltage of 100–120 kV, tube current of 100–300 mAs, section thickness of 0.625–1 mm, table

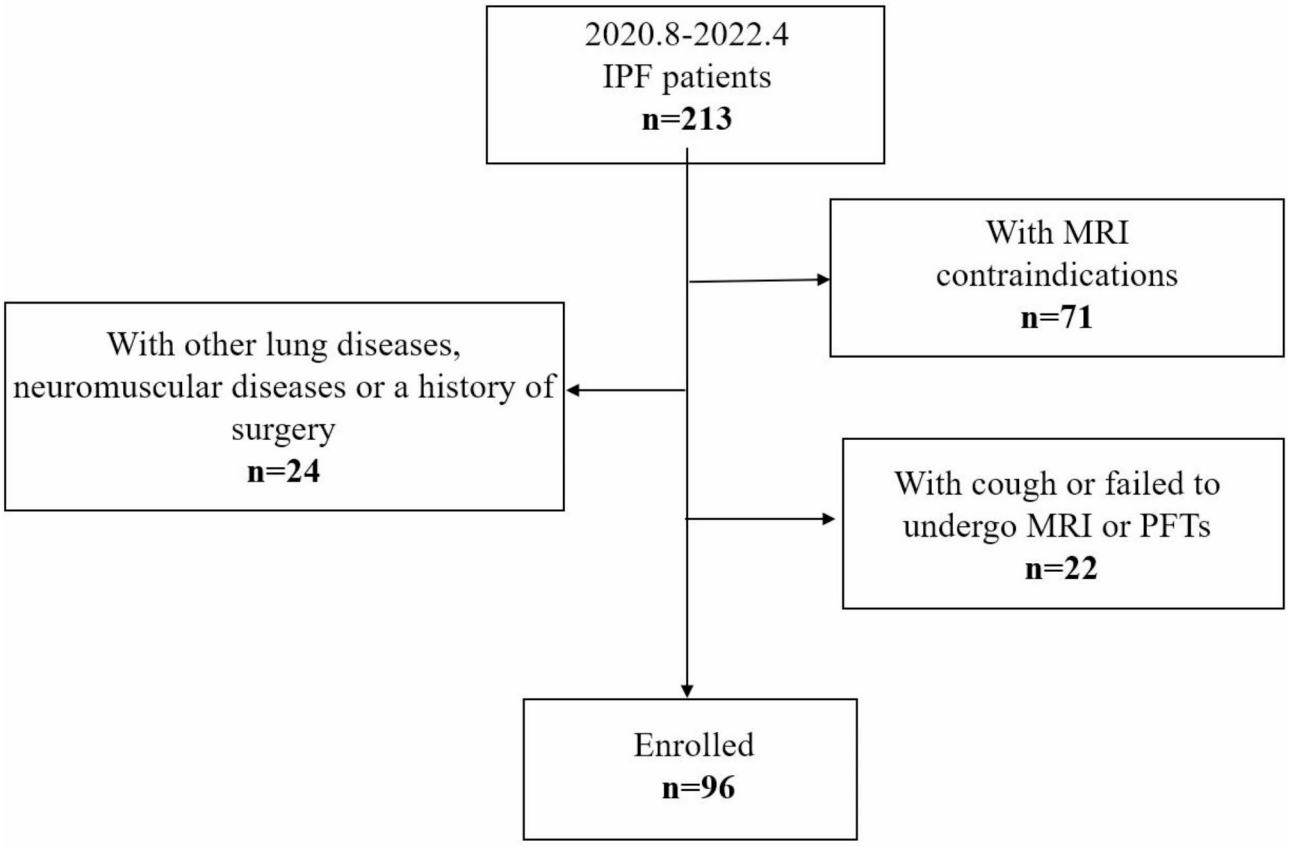

Fig. 1 The flowchart of inclusion and exclusion criteria of idiopathic pulmonary fibrosis (IPF) patients to this study

speed of 39.37 mm/s, gantry rotation time of 0.8 s, and reconstruction increment of 1–1.25 mm.

MRI protocol

Before the MRI scan, all participants were trained to practice quiet breathing and deep breathing in the supine position. Non-contrast chest MRI was performed on a 1.5T MRI scanner (MAGNETOM Aera; Siemens Healthcare, Erlangen, Germany) with an 18-channel phased-array body coil and 12-channel spine coil. To monitor whether subjects cooperated with breathing instructions (quiet breathing and deep breathing), the respiratory cushion was attached to the right upper abdomen using the respiratory belt. Free-breathing Dynamic MRI(D-MRI) was acquired using a 2D dynamic fast spoiled gradient-recalled echo sequence with parallel imaging acceleration($r = 2$). The key parameters were as follows: TR = 868ms; TE = 46ms; Flip Angle = 160°; FOV = 340 × 340 mm; resolution = 0.8 × 0.8 × 10.0 mm. A total of 40 frames for each slice were sampled with a time of 16s.

According to Yang et al. [19], D-MRI was respectively obtained in one coronal, one right sagittal, and three transversal planes during free quiet-breathing and free deep-breathing with a breathing navigator to monitor the respiratory situation (Fig. 2). The transversal images were respectively acquired at the level of the aortic arch, tracheal carina, and the right diaphragmatic dome which represent the upper, middle, and lower part of the chest wall (Supplement Fig. 1). The coronal and sagittal images were obtained in a coronal plane through tracheal bifurcation, and a right sagittal plane passing through the lung apex and right diaphragmatic dome (Supplement Fig. 1), respectively. For each imaging plane, D-MRI acquired the cine of respiratory muscle motion of multiple breathing cycles in both quiet breathing (16 s) and deep breathing (16 s) without reathing hold. The total scanning time including quiet breathing and deep breathing in one coronal, one right sagittal, and three transversal planes is 160s.

Segmentation of MR images

Each frame on the transversal, coronal, and sagittal planes among two to four respiratory cycles was manually segmented by two cardiothoracic radiologists with 20 years and 7 years of experience together using InferScholar (https://www.infervision.com/). Lung was extracted from each plane along the inner chest wall (Fig. 2). Both the anteroposterior diameter (AP) and left to right transversal diameter (left-right, LR) were measured on three

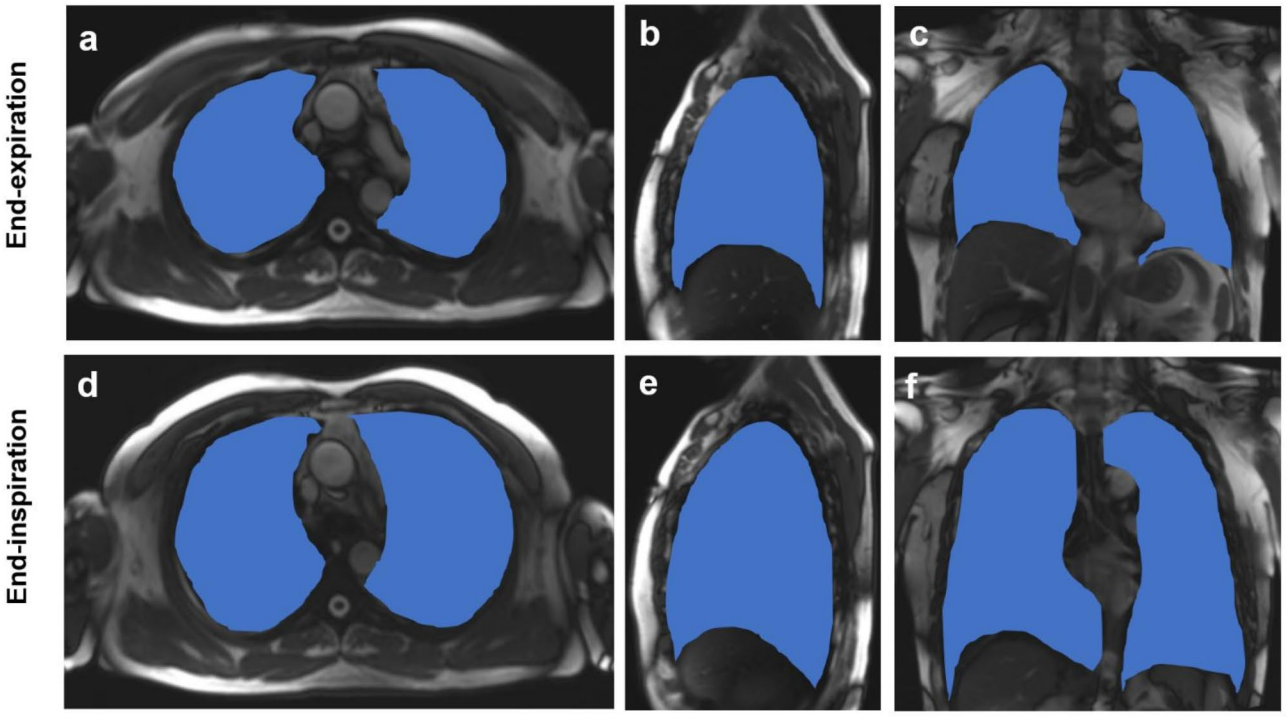

Fig. 2 Segmentation of dynamic MRI. Lung on the transversal plane in end-expiration(**a**) and end-inspiration(**d**) were segmented along the inner chest wall. Right lung on the sagittal plane in end-expiration(**b**) and end-inspiration(**e**) were segmented along the inner chest wall. Lung on the coronal plane in end-expiration(**c**) and end-inspiration(**f**) were segmented along the inner chest wall

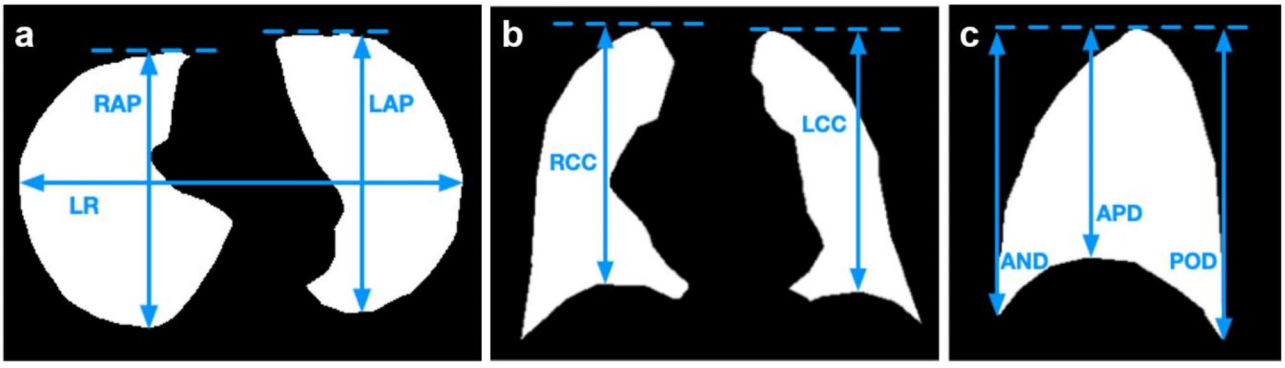

Fig. 3 Chest wall and diaphragm dimensions on MRI analyses. The anteroposterior diameter (AP) and transversal diameter (left-right, LR) were measured on the transversal plane(**a**). The height of thorax was measured on the coronal cranial-caudal directions (CC) (**b**). The distance between the lung apex and anterior diaphragm (AND), diaphragm apex (APD), and posterior diaphragm (POD) on sagittal plane(**c**). R/LAP = the anterior-posterior distance of right and left lung, LR = the left-right distance, R/LCC = the cranial-caudal distance of right and left lung on coronal plane

transversal slices (Fig. 3a). The height of the thorax was measured on the coronal cranial-caudal directions (CC) (Fig. 3b and c) [12, 19, 20].

Evaluation of the motion of the chest wall

The motion of the chest wall during quiet breathing and deep breathing was respectively by right and left AP ratio, LR ratio, and thoracic area ratio at the end-inspiration and end-expiration on three transversal planes at the aortic arch, tracheal carina, and the right diaphragmatic dome levels [12, 19, 20]. The AP is defined as the longest distance between the anterior inner chest wall and the posterior inner chest wall and the LR is defined as the longest distance between the right inner chest wall and the left inner chest wall (Fig. 3a). We calculated right and left AP, LR, and thoracic area ratios by dividing end-inspiration data by end-expiration data.

Evaluation of diaphragmatic motion

The diaphragmatic motion was evaluated with the left and right cranial-caudal (CC) distance measured as the distance between the lung apex and diaphragmatic dome

on the coronal slice [19] (Fig. 3b). Furthermore, the distance between the lung apex and the anterior diaphragm (AND), diaphragm apex (APD), and posterior diaphragm (POD) on the sagittal plane was also measured (Fig. 3c). Moreover, to evaluate the shape of the diaphragm, the area below the diaphragmatic curvature (DA) and the height of the diaphragmatic curvature (DH) was measured to calculate the DA ratio and DH ratio at the end-inspiration and end-expiration on the right diaphragm (Fig. 4). The DA is the area between the diaphragm and the line connecting between the anterior and posterior diaphragmatic corners and the DH is the perpendicular distance between the diaphragm apex and the line connecting between the anterior and posterior diaphragmatic angle.

Quantification of fibrosis on HRCT

According to Sun et al. [21, 22], lung segmentation was performed with the software InferScholar (https://www.infer-vision.com/) and manually corrected by one 15-year experienced chest radiologist. Then ground-glass opacities (GGO), reticulation, and honeycombing signs on HRCT were manually outlined in each CT slice, as shown in Supplement Fig. 2. The extent of fibrosis was expressed as the percentage of segmented reticulation and honeycombing signs in the total lung volume (TLV).

Statistical analysis

All statistical analyses were performed with SPSS 26.0 (IBM Corp, Armonk, NY, USA). Data were assessed for normal distribution before further statistical calculations. Normally distributed data are presented as mean ± SD and non-normally distributed data are presented as median with interquartile ranges. Data of IPF patients and healthy controls were compared in an unpaired t-test and Mann-Whitney U test for continuous variables and Fisher's exact test or chi-square test for categorical variables. The Spearman correlation coefficient was used to calculate the association between the clinical and MRI metrics. The intraclass coefficients (ICC) were used to determine the inter-observer agreement. ICCs were classified from null (= 0) to very good (> 0.80) and almost perfect (> 0.95) [23]. The significance level was set at $p \le 0.05$.

Results

Baseline characteristics of all participants

Ninety-six patients with IPF (92 men, mean age: 61 ± 7 years) and 50 healthy controls (46 men, mean age: 58 ± 6 years) were enrolled. Demographic and clinical data of IPF patients and healthy controls are depicted in Table 1. In comparison to healthy controls, the TLV of IPF patients was significantly reduced (4.3 ± 0.9 L vs. 4.7 ± 0.5 L, $p = 0.013$). The mean values of FVC% predicted (82.9 ± 16.6), and FEV1% (86.0 ± 15.8) predicted of IPF patients were worse than those of healthy controls. Moreover, the TLC% predicted (69.4 ± 13.9) and DLco% predicted (54.9 ± 17.3) of IPF patients were significantly lower than healthy controls. The 6MWD of IPF patients was 495.5 ± 74.7 m which was significantly worse than the normal controls (775.6 ± 49.5 m, $p < 0.001$). Dyspnea score was in MRC 1(47.9%) MRC 2(41.7%) and MRC 3 (10.4%). The extent of fibrosis of IPF measured on HRCT was19.8 ± 11.3%.

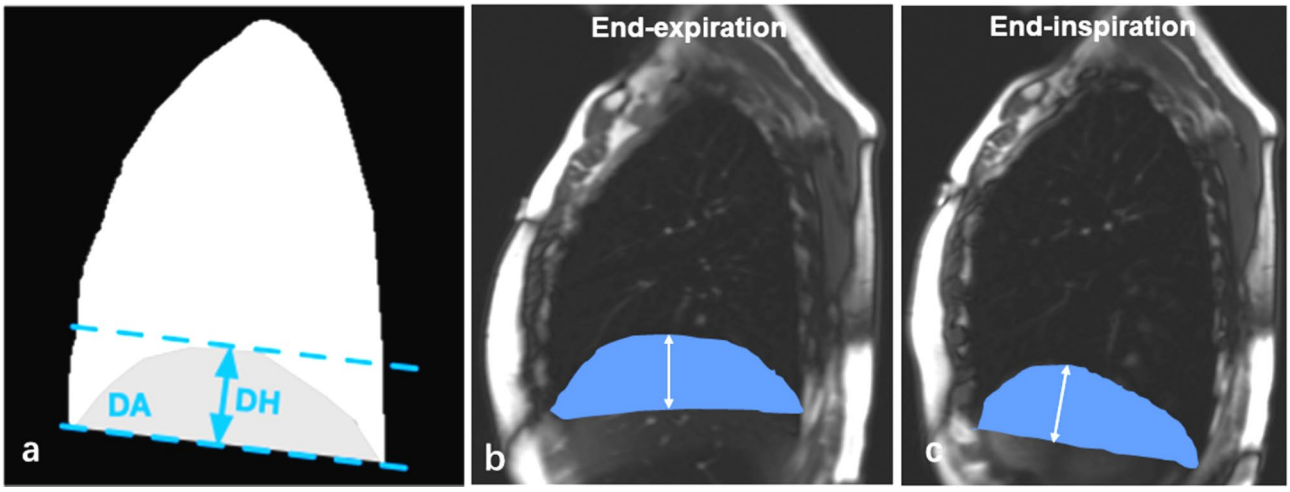

Fig. 4 Measurements of the height (DH) and area (DA) of the diaphragm curvature (**a**). The height of the diaphragm (DH) was measured to calculate the DA ratio and DH ratio. The DA is the area between the diaphragm and the line connecting the anterior and posterior diaphragmatic corners and the DH is the perpendicular distance between the diaphragm apex and the line connecting between the anterior and posterior diaphragmatic angle between end-inspiration and end-expiration on the right diaphragm(**a**). Measurements of the height (DH) and area (DA) of the diaphragm curvature in end-expiration(**b**) and end-inspitation(**c**)

Table 1 The characteristics of all participants

patients	IPF(*N* = 96)	Control(*N* = 50)	T/F	*P*
Mean age(range)	61 ± 7	58 ± 6	2.819	0.057
Gender, male, n (%)	92(95.8%)	46(92.0%)	0.002	0.962
Smoking, n (%)	80(83.3%)	16(32.0%)	4.587	<0.001
Height(cm)	168.1 ± 5.9	169.5 ± 6.4	-1.370	0.173
Weight(kg)	72.9 ± 9.1	71.00 ± 8.2	1.259	0.210
BMI(m/kg^2)	25.8 ± 2.6	24.7 ± 2.3	1.792	0.077
TLV on HRCT (L)	4.3 ± 0.9	4.7 ± 0.5	-2.511	0.013
Pulmonary function				
FVC % predicted	82.9 ± 16.6	103.3 ± 11.0	-7.895	<0.001
FEV1% predicted	86.0 ± 15.8	99.1 ± 12.5	-5.118	<0.001
FEV1/FVC% predicted	82.6 ± 5.9	83.1 ± 9.9	-0.340	0.734
TLC% predicted	69.4 ± 13.9	98.5 ± 9.7	-13.325	<0.001
DLCO % predicted	54.9 ± 17.3	100.0 ± 14.1	-15.976	<0.001
6MWD(m)	495.5 ± 74.7	775.6 ± 49.5	-12.405	< 0.001
Resting dyspnea (MRC), n (%)				
1	46(47.9%)	\		
2	40(41.7%)	\		
3	10(10.4%)	\		
4	0	\		
5	0	\		
HRQoL				
Respiratory symptoms	42.6 ± 23.7	\		
Activity	51.8 ± 74.3	\		
Psychosocial impact	19.5 ± 17.6	\		
Total	30.0 ± 17.3	\		
GAP score, n (%)				
I	66(45.2%)	\		
II	26(17.8%)	\		
III	4(2.7%)	\		
HRCT, n (%)				
UIP	78(81.3%)	\		
Possible UIP	18(18.7%)	\		
The percentage of ILD findings on HRCT				
GGO (%)	0.18 ± 0.9	\		
Reticulation (%)	11.1 ± 8.9	\		
Honeycombing (%)	8.7 ± 10.3	\		
Pulmonary fibrosis (%)	19.8 ± 11.3	\		

NOTE: IPF, idiopathic pulmonary fibrosis; BMI, body mass index; TLV: total lung volume from HRCT; FEV1, forced expiratory volume; FVC, forced vital capacity; TLC, total lung capacity; DLCO, diffusing capacity of the lungs for carbon monoxide; 6 MWD, 6 min-walk distance; UIP, usual interstitial pneumonia; GAP, gender-age-physiology variables (FVC and DLco); GGO, ground-glass opacity

Evaluation of chest wall function

Table 2 indicated that the median AP ratio, LR ratio, and lung area ratio on three transversal planes during quiet breathing were comparable between IPF patients and the control group ($p > 0.05$). During deep breathing, the median AP ratios on three transversal planes of IPF patients significantly decreased in comparison with the control group. Meanwhile, the median lung area ratios of IPF patients on the aortic arch, tracheal carina, and right diaphragmatic dome, respectively were also lower than those of healthy controls (1.16vs 1.26, $p<0.001$; 1.11vs 1.19, $p<0.001$; 1.09 vs. 1.16, $p<0.001$). However, the median LR ratio was similar between the IPF and control group at each transversal plane during deep breathing. The ICC were as follows: quiet breathing: AP ratio: ICC = 0.98; LR ratio: ICC = 0.95; lung area ratio on 3 transversal planes: ICC = 0.82; ICC = 0.91; ICC = 0.88. Deep breathing: AP ratio: ICC = 0.96;LR ratio: ICC = 0.98; lung area ratio on 3 transversal planes: ICC = 0.88; ICC = 0.89; ICC = 0.86.

Evaluation of diaphragmatic function

The diaphragmatic motion of the IPF and control group during quiet and deep breathing were shown in Supplement Figs. 3 and 4. Table 3 shows that the median CC ratios, DA, DH, and lung area ratios in patients with IPF were comparable to healthy controls during quiet breathing. During deep breathing, the median CC ratios of IPF patients on the coronal plane were lower than those of healthy controls(left thorax 1.20 vs. 1.34, $p<0.001$; right thorax 1.28 vs. 1.42, $p<0.001$) (Fig. 5). The median lung area ratio of IPF patients decreased in comparison with the control group (1.56 vs. 1.76, $p<0.002$). Meanwhile, the median lung area ratio of IPF patients was lower than healthy controls (1.38 vs. 1.60, $p<0.001$). Moreover, the median DH and DA ratios of IPF patients were higher than healthy controls (DH: 0.96 vs. 0.81, $p<0.001$; DA: 1.00 vs. 0.90, $p<0.001$). The ICC between manual measurements was good (Quiet breathing, CC ratios ICC = 0.84, DA ICC = 0.87, DH ICC = 0.91, lung area ratio ICC = 0.88; Deep breathing, CC ratios ICC = 0.89, DA ICC = 0.86, DH ICC = 0.90, lung area ICC = 0.91).

Furthermore, the thoracic area-time curves in the coronal and sagittal planes (Fig. 6) indicated that the amplitude of diaphragm movement during quiet breathing in IPF patients was slightly lower than that in the control group (Fig. 6a and b). However, the amplitude of diaphragm movement during deep breathing in IPF patients was significantly lower than that in the control group (Fig. 6c and d). By comparing the amplitude of motion curves between two groups during quiet and deep breathing, the mobility reserve of respiratory muscles in IPF patients significantly reduced.

Table 2 Comparison of chest wall motion on three transversal planes on dynamic MRI between IPF patients and control group

Ratios	Quiet breathing			Deep breathing		
	Controls	IPF	*P*	Controls	IPF	*P*
The arcus aortae level						
Left AP	1.02 (1.01, 1.05)	1.02 (1.01, 1.03)	0.151	1.17 (1.12, 1.25)	1.11 (1.06, 1.18)	<0.001*
Right AP	1.01 (0.99, 1.03)	1.02 (1.00, 1.03)	0.252	1.15 (1.12, 1.22)	1.09 (1.06, 1.14)	<0.001*
LR	1.01 (1.00, 1.02)	1.01 (1.00, 1.02)	0.432	1.06 (1.04, 1.08)	1.04 (1.02, 1.08)	0.067
Area	1.02 (1.01, 1.04)	1.02 (1.01, 1.04)	0.252	1.26 (1.16, 1.34)	1.16 (1.08, 1.27)	<0.001*
The tracheal carina level						
Left AP	1.01 (1.01, 1.02)	1.02 (1.01, 1.04)	0.054	1.14 (1.08, 1.18)	1.09 (1.06, 1.14)	0.004*
Right AP	1.01 (1.00, 1.03)	1.01 (1.01, 1.02)	0.322	1.13 (1.07 1.17)	1.07 (1.04, 1.11)	<0.001*
LR	1.01 (1.00, 1.01)	1.01 (1.00, 1.01)	0.462	1.04 (1.03, 1.05)	1.03 (1.02, 1.05)	0.068
Area	1.02 (1.01, 1.03)	1.02 (1.01, 1.03)	0.864	1.19 (1.12 1.28)	1.11 (1.06, 1.17)	<0.001*
The diaphragm dome level						
Left AP	1.02 (1.01,1.03)	1.01 (1.01, 1.02)	0.092	1.12 (1.06, 1.15)	1.07 (1.03, 1.09)	<0.001*
Right AP	1.01 (1.00, 1.02)	1.01 (1.01, 1.02)	0.056	1.10 (1.06, 1.12)	1.06 (1.04, 1.09)	<0.001*
LR	1.00 (1.00, 1.01)	1.00 (1.00, 1.01)	0.527	1.03 (1.02, 1.05)	1.03 (1.02, 1.05)	0.438
Area	1.01 (1.00, 1.02)	1.01(1.00, 1.02)	0.051	1.16 (1.08, 1.22)	1.09 (1.06, 1.15)	<0.001*

NOTE: *$p < 0.05$. IPF, idiopathic pulmonary fibrosis; AP, anterior-posterior (AP) distance; LR, left-right (LR) distance

Table 3 Comparison of diaphragm motion of dynamic MRI between IPF patients and control group

Ratios	Quiet breathing			Deep breathing		
	Controls	IPF	*P*	Controls	IPF	*P*
The coronal plane						
Left CC	1.08 (1.07, 1.10)	1.08 (1.06, 1.11)	0.905	1.34 (1.24, 1.48)	1.20 (1.15, 1.30)	<0.001*
Right CC	1.09 (1.07, 1.12)	1.10 (1.07, 1.12)	0.505	1.42 (1.29, 1.55)	1.28 (1.17, 1.36)	<0.001*
Area	1.15 (1.12, 1.18)	1.18 (1.13, 1.27)	0.057	1.76 (1.55, 2.02)	1.56 (1.41, 1.73)	<0.002*
The right sagittal plane						
AND	1.04 (1.02,1.06)	1.04 (1.02, 1.06)	0.297	1.11 (1.08, 1.23)	1.10 (1.05, 1.16)	0.062
APD	1.08 (1.06,1.10)	1.09 (1.06, 1.10)	0.946	1.30 (1.21, 1.42)	1.20 (1.13, 1.26)	<0.001*
POD	1.08 (1.07, 1.11)	1.09 (1.07, 1.11)	0.831	1.32 (1.21, 1.38)	1.23 (1.16, 1.29)	<0.001*
Area	1.12 (1.09, 1.16)	1.12 (1.10, 1.15)	0.932	1.60 (1.36, 1.73)	1.38 (1.25, 1.50)	<0.001*
DH	0.97 (0.92, 1.02)	0.96 (0.92, 1.00)	0.798	0.81 (0.78, 0.97)	0.96 (0.88, 1.02)	<0.001*
DA	0.98 (0.96, 1.02)	0.98 (0.96,1.02)	0.228	0.90 (0.76, 1.02)	1.00 (0.89, 1.11)	<0.001*

Note: *$p < 0.05$.IPF, idiopathic pulmonary fibrosis; CC, the cranial-caudal distance; DH, the height of diaphragm; DA, the area of diaphragm; AND, APD, POD, the distance between the lung apex and anterior Diaphragm, Diaphragm apex, and posterior Diaphragm on sagittal plane, respectively

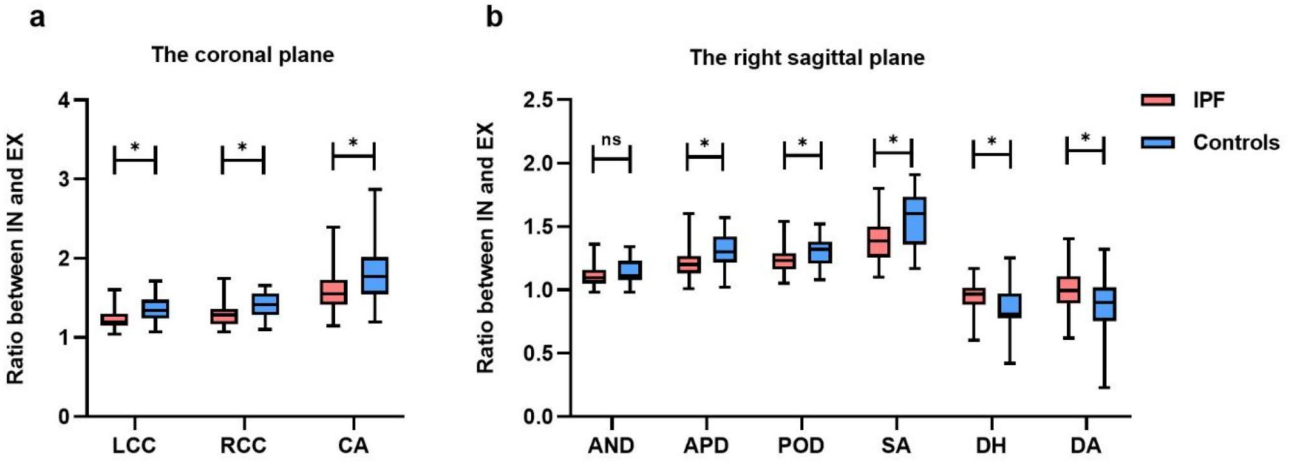

Fig. 5 The box showed the difference of ratios between inspiration(IN) and expiration(EX) among idiopathic pulmonary fibrosis (IPF) patients and healthy controls about diaphragm-related outcomes on the coronal(**a**) and sagittal planes(**b**). The cranial-caudal distance of right and left lung on coronal plane(R/LCC). The lung area on the coronal plane(CA). The distance between the lung apex and anterior (AND), apex (APD), and posterior (POD) of diaphragm on sagittal plane. The lung area on the coronal plane(SA). The height (DH) and area (DA) of the diaphragm curvature. *indicated $p<0.05$

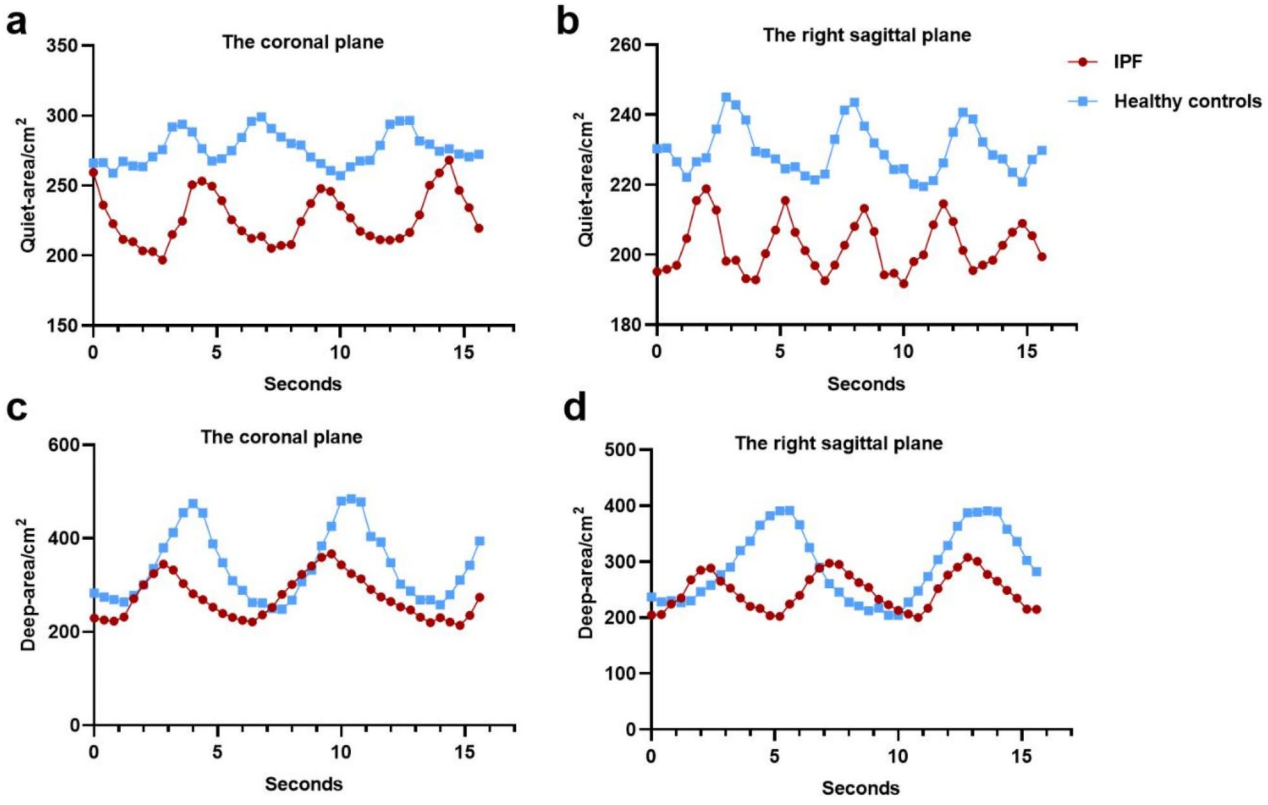

Fig. 6 The thoracic area time curves during quiet breathing and deep breathing. The coronal curve amplitude of idiopathic pulmonary fibrosis (IPF) patients during quiet breathing is slightly lower than that of the control group(**a**). The sagittal curve amplitude of IPF patients during quiet breathing is slightly lower than that of the control group(**b**). The coronal curve amplitude of IPF patients during deep breathing is significantly lower than that of the control group(**c**). The sagittal curve amplitude of IPF patients during deep breathing is significantly lower than that of the control group(**d**)

Correlations of diaphragmatic and chest wall function with severity of IPF patients

Table 1 shows that TLV on HRCT in patients with IPF was smaller than in normal controls (t=-2.511, $p=0.013$). Table 4 indicates that the AP ratios, CC ratios, and lung areas ratios of each plane during deep breathing correlated with TLV on HRCT (0.208–0.488, $p<0.05$), FVC% predicted(0.227–0.467, $p<0.05$), FEV1% predicted (0.276–0.462, $p<0.05$), TLC% predicted (0.264–0.453, $p<0.05$), DLco% predicted (0.240–0.445, $p<0.05$) and 6MWD (0.305–0.481, $p<0.05$). In addition, the DH and DA ratios of the diaphragm during deep breathing negatively correlated with TLV (DH: $r=-0.306$, $p<0.05$; DA: $r=-0.281$, $p<0.05$), FVC% predicted (DH: $r=-0.385$, $p<0.01$; DA: $r=-0.347$, $p<0.01$), FEV1% predicted (DH: $r=-0.429$, $p<0.01$; DA: $r=-0.378$, $p<0.01$), TLC% predicted (DH: $r=-0.395$ $p<0.01$; DA: $r=-0.398$, $p<0.01$), and DLco% predicted (DH: $r=-0.309$, $p<0.01$; DA: $r=-0.270$, $p<0.05$). However, neither diaphragmatic nor chest wall motion metrics correlated with the extent of fibrosis on HRCT (Supplement Table 1). Table 5 shows that the median LR and lung area ratios, right CC ratio, and APD in IPF patients were significantly different between MRC 1, MRC 2, and MRC3. However, neither diaphragmatic nor chest wall motion metrics correlate with HRQoL (Supplement Table 1).

Discussion

In this study, we conducted a detailed evaluation of diaphragmatic and chest wall motion in IPF patients using Dyn-MRI and there several findings as follow: (I) the motion of the diaphragm and chest wall during deep breathing in IPF patients had a significant reduction when compared to the control group. (II) The motion metrics of the diaphragm and chest wall during the deep breathing were found to be correlated with TLV, FVC%, FEV1%, TLC%, and DLco%; (III) The motion metrics of the diaphragm and chest wall during deep breathing showed correlations with 6-MWD and the level of dyspnea of IPF patients.

The diaphragm is the main breathing muscle and the normal diaphragmatic motion is vital for ventilation. In ILD, diaphragm dysfunction is related to hypoxia, malnutrition, and overload due to the increased elastic recoil of the lung [2, 24]. By ultrasound or CT, Savtana et al. showed the diaphragmatic motion in ILD patients was

Table 4 Correlations between motion metrics and pulmonary function in IPF patients

		TLV (L)	6MWD(m)	FVC%	FEV1%	TLC%	DLco%
Chest Wall motional metrics							
AAL	Left AP	0.347**	0.469**	0.434**	0.377**	0.386**	0.327**
	Right AP	0.355*	0.464*	0.454**	0.383**	0.371**	0.299*
	LR	0.334*	0.413*	0.278*	0.278*	0.267*	0.240*
	Area	0.466**	0.447**	0.458**	0.406**	0.329**	0.375**
TCL	Left AP	0.355**	0.353*	0.259*	0.309*	0.267*	0.240*
	Right AP	0.512**	0.305*	0.472**	0.425**	0.453**	0.367**
	LR	0.188	0.443*	0.227	0.161	0.206	0.367**
	Area	0.444**	0.463**	0.458**	0.410*	0.265*	0.389**
LDL	Left AP	0.208*	0.401**	0.279*	0.276*	0.264*	0.171
	Right AP	0.425**	0.398**	0.388**	0.416**	0.385**	0.395**
	LR	0.366*	0.417**	0.164	0.104	0.104	0.109
	Area	0.488**	0.481**	0.467**	0.462**	0.422**	0.347**
Diaphragm motional metrics							
CP	Left CC	0.342**	0.269*	0.391**	0.351**	0.345**	0.445**
	Right CC	0.292*	0.217*	0.366**	0.341**	0.328**	0.434**
	Area	0.383**	0.383*	0.329**	0.276**	0.269*	0.400*
RSP	AND	0.167	0.167	0.143	0.153	0.169	0.145
	APD	0.205	0.205*	0.335**	0.350**	0.359**	0.340**
	POD	0.341*	0.341*	0.325**	0.333**	0.305*	0.320**
	Area	0.390**	0.390**	0.403**	0.416**	0.391**	0.429**
	DH	-0.306*	0. 240*	-0.385**	-0.429**	-0.395**	-0.309**
	DA	-0.281*	0.138	-0.347**	-0.378**	-0.398**	-0.270*

Note: * indicated $p<0.05$; ** indicated $P<0.01$.TLV, total lung volume; 6-MWD, 6 min-walk distance; FVC, forced vital capacity; FEV1, forced expiratory volume; TLC, total lung capacity; DLCO, diffusing capacity of the lungs for carbon monoxide; AAL, the arcus aortae level; TCL, the tracheal carina level; LDL, the liver dome level; CP, the coronal plane; RSP, the right sagittal plane. AP, anterior-posterior (AP) distance; LR, left-right (LR)distance; CC, the cranial-caudal distance; AND, APD, POD, the distance between the lung apex and anterior, apex, and posterior of diaphragm on sagittal plane, respectively. DH, the height of diaphragm; DA, the area of diaphragm

reduced, compared to the healthy controls during the deep breathing [7, 25, 26]. However, by ultrasound, He et al. found that the motion of the diaphragm was similar between IPF patients and healthy controls [27]. By Dyn-MRI, our results indicated that the diaphragmatic motion was decreased during deep breathing in IPF patients, compared with the normal control. Furthermore, we also found that the reduced motion of the diaphragm in IPF patients was prominent in the posterior diaphragm and diaphragm apex, but not in the anterior diaphragm. This is consequent to lower APD and POD values in patients with IPF, particularly in cases with more severe symptoms. Moreover, this also may be related to the distribution of fibrosis, because the fibrosis of IPF is most severe in subpleural regions of the lower lung, especially prominent in the dorsal side of the lung bottom and the contribution of central and posterior diaphragm motion to ventilation is higher than the anterior part of the diaphragm [20]. Moreover, the area below the diaphragmatic curvature (DA) and the height of the diaphragmatic curvature (DH) in IPF patients during deep inspiration are higher than those in the control group, which may be explained by the progressively reduced lung volume of IPF leading to a lower flattening of the diaphragm during inspiration and a globally limited excursion [7]. In contrast, the diaphragmatic curvature of COPD patients was decreased and demonstrated more flattening due to increased lung volume because of air trapping and airway obstruction [28, 29].

According to a previous study [30], diaphragmatic mobility was found to increase during quiet breathing in COPD patients. In contrast, diaphragm motion during quiet breathing in IPF patients was comparable to that of control individuals. However, the amplitude of thoracic area-time curves in IPF patients decreased, particularly during deep breathing. By comparing the amplitude of motion curves between the two groups during quiet and deep breathing, we found a significant reduction of the motion reserve in the respiratory muscles of IPF patients which has not been reported in previous study. This may be attributed to the increased lung elastic recoil experienced in IPF, which places an excessive burden on the respiratory muscles during deep breathing.

In addition to diaphragmatic motion, chest wall motion also plays a role in active ventilation. However, there have been few studies exploring the relationship between chest wall motion and the severity of IPF. We observed a significant reduction in chest wall motion in the dorsal-ventral (anteroposterior) direction during deep breathing in IPF patients, which is in line with findings from a

Table 5 Diaphragm and chest wall motion in IPF patients with the score of dyspnea

Patients		MRC = 1 (*N* = 46)	MRC = 2 (*N* = 40)	MRC = 3 (*N* = 10)	F/(*P*)
Chest wall functional metrics					
AAL	Left AP ratio	1.11(1.05, 1.20)	1.11(1.06, 1.18)	1.12(1.07, 1.18)	1.643 (0.440)
	Right AP ratio	1.09(1.06, 1.13)	1.10(1.06, 1.17)	1.11(1.08, 1.22)	8.761 (0.013) *
	LR ratio	1.07(1.02, 1.10)	1.04(1.01, 1.07)	1.03(1.02, 1.08)	6.859 (0.032) *
	Area ratio	1.18(1.09, 1.34)	1.15(1.06, 1.28)	1.16(1.13, 1.28)	11.301 (0.004) *
CL	Left AP ratio	1.09(1.06 1.15)	1.09(1.07, 1.14)	1.09(1.07, 1.13)	0.012 (0.994)
	Right AP	1.09(1.04, 1.11)	1.07(1.03, 1.11)	1.07(1.06, 1.11)	3.476 (0.176)
	LR ratio	1.03(1.01, 1.05)	1.03(1.02, 1.05)	1.03(1.02, 1.05)	4.188(0.123)
	Area ratio	1.15(1.06, 1.25)	1.12(1.06, 1.16)	1.11(1.08, 1.16)	7.046 (0.030) *
DDL	Left AP ratio	1.07(1.04, 1.10)	1.06(1.02, 1.09)	1.06(1.02, 1.09)	1.395 (0.498)
	Right AP ratio	1.06(1.04, 1.09)	1.06(1.03, 1.08)	1.06(1.03, 1.08)	3.777 (0.151)
	LR ratio	1.03(1.02, 1.06)	1.03(1.02, 1.05)	1.03(1.02, 1.05)	3.434(0.180)
	Area ratio	1.12(1.06, 1.17)	1.09(1.03, 1.12)	1.10(1.06, 1.12)	9.615 (0.008) *
Diaphragm functional metrics					
CP	Left CC ratio	1.21(1.13, 1.38)	1.20(1.15, 1.25)	1.20 (1.15, 1.25)	1.065(0.587)
	Right CC ratio	1.31(1.17, 1.39)	1.27(1.15, 1.31)	1.18 (1.14, 1.25)	9.091 (0.011) *
RSP	AND ratio	1.10(1.04, 1.20)	1.09(1.05, 1.14)	1.08 (1.05, 1.14)	5.175(0.075)
	APD ratio	1.23(1.13, 1.29)	1.19(1.12, 1.24)	1.20 (1.10, 1.25)	7.211 (0.027) *
	POD ratio	1.24(1.18, 1.31)	1.21(1.15, 1.27)	1.23(1.16, 1.28)	4.116(0.128)
	DH ratio	0.98(0.88, 1.04)	0.93(0.89, 1.00)	0.95 (0.87, 1.00)	2.501(0.286)
	DA ratio	0.96(0.87, 1.11)	1.03(0.91, 1.11)	1.06 (0.93, 1.13)	6.353 (0.052)

Note: *$p < 0.05$.IPF, idiopathic pulmonary fibrosis; AAL, the arcus aortae level; CL, the tracheal carina level; DDL, the diaphragm dome level; CP, the coronal plane; RSP, the right sagittal plane. AP, anterior-posterior (AP) distance; LR, left-right (LR) distance; CC, the cranial-caudal distance; AND, APD, POD, the distance between the lung apex and anterior, apex, and posterior of diaphragm on the sagittal plane, respectively; DH, the height of diaphragm; DA, the area of diaphragm

study that utilized HRCT [26]. This can be explained by the fact that the primary motion of the chest wall during the respiratory cycle occurs in the dorsal ventral direction [19, 31].

In healthy volunteers [32–35] and patients with COPD [36], diaphragm motion has been shown to correlate with pulmonary function. In IPF patients, we found that both the diaphragm and chest wall functional metrics during deep breathing measured using Dyn-MRI, were associated with FVC%, FEV1%, and TLC%. Additionally, there was a negative correlation between increased diaphragmatic curvature and TLV, FVC%, FEV1%, and TLC%. These findings suggest that diaphragm and chest wall dysfunction correlate with PFTs in IPF patients.

Diaphragmatic weakness is associated with respiratory symptoms, especially exercise intolerance, dyspnea, sleep disturbances, and in the most severe cases, a negative impact on survival [37]. By diaphragmatic ultrasound, Santana PV et al. suggested that the lower diaphragmatic mobility during deep breathing correlated to increased dyspnea, worse HRQoL, and lung function in patients with fibrotic ILD [25]. In this study, the decreased diaphragm and chest wall motion correlated with the reduced 6MWD and severe dyspnea. These indicated respiratory muscle dysfunction correlated with the severity of IPF patients. Although impaired HRQoL was observed in FILD patients, our study did not find a correlation between diaphragmatic or chest wall motion metrics and HRQoL. This may be attributed to the absence of patients with poorer HRQoL in our population. Moreover, there was no significant correlation between diaphragmatic and chest wall functional metrics and the extent of pulmonary fibrosis, suggesting that the dysfunction of respiratory muscles in IPF patients is not solely influenced by the extent of fibrosis in the lungs. Other factors such as hypoxia, exercise intolerance, and malnutrition may contribute to the impaired function of respiratory muscles in IPF patients. It highlights the complex nature of respiratory muscle dysfunction in IPF and the need to consider multiple factors when assessing its impact.

There are several limitations of this study. This is a single-center observational study, the distribution of cases is unbalanced, such as a lack of patients with severe dyspnea (MRC = 4 or 5) or poor HRQoL which may limit the generalizability of results. Another limitation was that we did not measure diaphragm thickness and force, the correlation of diaphragm thickness and force with diaphragmatic motion remains unknown. In addition, Dyn-MRI was obtained in the supine position and PFTs were obtained in the sitting position which may weaken the correlation of respiratory muscle function and pulmonary function. The correlation of respiratory muscle dysfunction with the prognosis of IPF patient needs further observation. Finally, the therapy with steroids may certainly cause respiratory muscle weakness, while the details about special treatment in IPF patients were limited in this study. Together with the other potential confounders, such as smoking will also be studied in the future with larger sample sizes.

Conclusions

Patients with IPF exhibited a significantly reduced motion of the posterior diaphragm, diaphragm apex, and chest wall in the dorsal-ventral direction during the deep breathing. Additionally, the weaker diaphragm and chest wall motion correlated with the clinical severity of IPF.

Supplementary Information

The online version contains supplementary material available at https://doi.org/10.1186/s12890-025-03572-6.

Supplementary Material 1

Author contributions

(1) the conception and design of the study: XY, ML, HD; (2) acquisition of data, analysis, and interpretation of data: XY, HW, LA, NY, WJ, HY, BX, JG, YR, RZ, ML; (3) drafting the article or revising it critically for important intellectual content: XY, ML, HD; (4) final approval of the version to be submitted: All authors.

Funding

This work was supported by National Key Technologies R & D Program Precision China (No. 2021YFC2500700; 2016YFC0901101) and National Natural Science Foundation of China (No. 81870056).

Data availability

Data is available on request from the authors. The data that support the fndings of this study are available from the corresponding author, [Min Liu.], upon reasonable request.

Declarations

Ethics approval and consent to participate

This study was approved by Institutional ethics committee of China-Japan Friendship Hospital(2019-123-K85-1). All participants provided written informed consent.

Competing interests

The authors declare no competing interests.

Author details

[1]Department of Pulmonary and Critical Care Medicine, General Hospital of Ningxia Medical University, Yinchuan, Ningxia 750004, China
[2]National Center for Respiratory Medicine, State Key Laboratory of Respiratory Health and Multimorbidity, National Clinical Research Center for Respiratory Diseases, Institute of Respiratory Medicine, Chinese Academy of Medical Sciences, Center of Respiratory Medicine, China-Japan Friendship Hospital, Beijing 100029, China
[3]Chinese Academy of Medical Sciences and Peking Union Medical College, Beijing 100730, China
[4]Department of Radiology, China-Japan Friendship Hospital, 2 Yinghua Dong Street, Chao Yang District, Beijing 100029, China
[5]China-Japan Friendship Hospital, Capital Medical University, Beijing 100029, China
[6]Academy for Multidisciplinary Studies, Capital Normal University, Beijing 100080, China
[7]Department of Pulmonary and Critical Care Medicine, Friendship Hospital, 2 Yinghua Dong Street, Chao Yang District, Beijing 100029, China

Received: 6 April 2024 / Accepted: 26 February 2025
Published online: 14 March 2025

References

1. Raghu G, Collard HR, Egan JJ, Martinez FJ, Behr J, Brown KK, Colby TV, Cordier JF, Flaherty KR, Lasky JA, et al. An official ATS/ERS/JRS/ALAT statement: idiopathic pulmonary fibrosis: evidence-based guidelines for diagnosis and management. Am J Respir Crit Care Med. 2011;183:788–824.
2. Panagiotou M, Polychronopoulos V, Strange C. Respiratory and lower limb muscle function in interstitial lung disease. Chron Respir Dis. 2016;13:162–72.
3. Moon SW, Choi JS, Lee SH, Jung KS, Jung JY, Kang YA, Park MS, Kim YS, Chang J, Kim SY. Thoracic skeletal muscle quantification: low muscle mass is related with worse prognosis in idiopathic pulmonary fibrosis patients. Respir Res 2019, 20.
4. Ebihara K, Iwanami Y, Yamasaki K, Takemura A, Sato N, Usui Y, Nakamura Y, Kishi K, Homma S, Ebihara S. Appendicular skeletal muscle mass correlates with Patient-Reported outcomes and physical performance in patients with idiopathic pulmonary fibrosis. Tohoku J Exp Med. 2021;253:61–8.
5. Molgat-Seon Y, Guler SA, Peters CM, Vasilescu DM, Puyat JH, Coxson HO, Ryerson CJ, Guenette JA. Pectoralis muscle area and its association with indices of disease severity in interstitial lung disease. Respir Med. 2021;186:106539.
6. Suzuki Y, Aono Y, Kono M, Hasegawa H, Yokomura K, Naoi H, Hozumi H, Karayama M, Furuhashi K, Enomoto N, et al. Cause of mortality and sarcopenia in patients with idiopathic pulmonary fibrosis receiving antifibrotic therapy. Respirology. 2021;26:171–9.
7. Santana PV, Prina E, Albuquerque AL, Carvalho CR, Caruso P. Identifying decreased diaphragmatic mobility and diaphragm thickening in interstitial lung disease: the utility of ultrasound imaging. J Bras Pneumol. 2016;42:88–94.
8. Yang X, Liu M, Duan J, Sun H, An J, Benkert T, Dai H, Wang C. Three-dimensional ultrashort echo time magnetic resonance imaging in assessment of idiopathic pulmonary fibrosis, in comparison with high-resolution computed tomography. Quant Imaging Med Surg. 2022;12:4176–89.
9. Kotani T, Minami S, Takahashi K, Isobe K, Nakata Y, Takaso M, Inoue M, Maruta T, Akazawa T, Ueda T, Moriya H. An analysis of chest wall and diaphragm motions in patients with idiopathic scoliosis using dynamic breathing MRI. Spine (Phila Pa 1976). 2004;29:298–302.
10. Mankodi A, Kovacs W, Norato G, Hsieh N, Bandettini WP, Bishop CA, Shimellis H, Newbould RD, Kim E, Fischbeck KH, et al. Respiratory magnetic resonance imaging biomarkers in Duchenne muscular dystrophy. Ann Clin Transl Neurol. 2017;4:655–62.
11. Reyes-Leiva D, Alonso-Perez J, Mayos M, Nunez-Peralta C, Llauger J, Belmonte I, Pedrosa-Hernandez I, Segovia S, Diaz-Manera J. Correlation between respiratory accessory muscles and diaphragm pillars MRI and pulmonary function test in Late-Onset Pompe disease patients. Front Neurol. 2021;12:621257.
12. Harlaar L, Ciet P, van Tulder G, Pittaro A, van Kooten HA, van der Beek N, Brusse E, Wielopolski PA, de Bruijne M, van der Ploeg AT, et al. Chest MRI to diagnose early diaphragmatic weakness in Pompe disease. Orphanet J Rare Dis. 2021;16:21.
13. Iwasawa T, Takahashi H, Ogura T, Asakura A, Gotoh T, Shibata H, Inoue T. Influence of the distribution of emphysema on diaphragmatic motion in patients with chronic obstructive pulmonary disease. Jpn J Radiol. 2011;29:256–64.
14. Hellebrandova L, Chlumsky J, Vostatek P, Novak D, Ryznarova Z, Bunc V. Airflow limitation is accompanied by diaphragm dysfunction. Physiol Res. 2016;65:469–79.
15. Shimada A, Kawata N, Sato H, Ikari J, Suzuki E, Anazawa R, Suzuki M, Masuda Y, Haneishi H, Tatsumi K. Dynamic quantitative magnetic resonance imaging assessment of areas of the lung during Free-Breathing of patients with chronic obstructive pulmonary disease. Acad Radiol. 2022;29(Suppl 2):S215–25.
16. Mahler DA, Weinberg DH, Wells CK, Feinstein AR. The measurement of dyspnea. Contents, interobserver agreement, and physiologic correlates of two new clinical indexes. Chest. 1984;85:751–8.
17. Zimmermann CS, Carvalho CR, Silveira KR, Yamaguti WP, Moderno EV, Salge JM, Kairalla RA, Carvalho CR. Comparison of two questionnaires which measure the health-related quality of life of idiopathic pulmonary fibrosis patients. Braz J Med Biol Res. 2007;40:179–87.
18. Laveneziana P, Albuquerque A, Aliverti A, Babb T, Barreiro E, Dres M, Dubé B-P, Fauroux B, Gea J, Guenette JA et al. ERS statement on respiratory muscle testing at rest and during exercise. Eur Respir J 2019, 53.
19. Yang X, Sun H, Deng M, Chen Y, Li C, Yu P, Zhang R, Liu M, Dai H, Wang C. Characteristics of diaphragmatic and chest wall motion in people with normal pulmonary function: A study with Free-Breathing dynamic MRI. J Clin Med 2022, 11.
20. Kondo T, Kobayashi I, Taguchi Y, Ohta Y, Yanagimachi N. A dynamic analysis of chest wall motions with MRI in healthy young subjects. Respirology. 2000;5:19–25.

21. Sun HLM, Kang H, Yang X, Zhang P, Zhang R, Dai H, Wang C. Quantitative analysis of high-resolution computed tomography features of idiopathic pulmonary fibrosis: a structure-function correlation study. Quant Imaging Med Surg. 2022;12:3655–65.
22. Christe A, Peters AA, Drakopoulos D, Heverhagen JT, Geiser T, Stathopoulou T, Christodoulidis S, Anthimopoulos M, Mougiakakou SG, Ebner L. Computer-Aided diagnosis of pulmonary fibrosis using deep learning and CT images. Invest Radiol. 2019;54:627–32.
23. Landis JR, Koch GG. The measurement of observer agreement for categorical data. Biometrics. 1977;33:159–74.
24. Moylan JS, Reid MB. Oxidative stress, chronic disease, and muscle wasting. Muscle Nerve. 2007;35:411–29.
25. Santana PV, Cardenas LZ, de Albuquerque ALP, de Carvalho CRR, Caruso P. Diaphragmatic ultrasound findings correlate with dyspnea, exercise tolerance, health-related quality of life and lung function in patients with fibrotic interstitial lung disease. BMC Pulm Med. 2019;19:183.
26. Kang JH, Choi J, Chae KJ, Shin KM, Lee CH, Guo J, Lin CL, Hoffman EA, Lee C. CT-derived 3D-diaphragm motion in emphysema and IPF compared to normal subjects. Sci Rep. 2021;11:14923.
27. He L, Zhang W, Zhang J, Cao L, Gong L, Ma J, Huang H, Zeng J, Zhu C, Gong J, et al. Diaphragmatic motion studied by M-mode ultrasonography in combined pulmonary fibrosis and emphysema. Lung. 2014;192:553–61.
28. Iwasawa T, Yoshiike Y, Saito K, Kagei S, Gotoh T, Matsubara S. Paradoxical motion of the hemidiaphragm in patients with emphysema. J Thorac Imaging. 2000;15:191–5.
29. Rochester DF, Braun NM. Determinants of maximal inspiratory pressure in chronic obstructive pulmonary disease. Am Rev Respir Dis. 1985;132:42–7.
30. Corbellini C, Boussuges A, Villafañe JH, Zocchi L. Diaphragmatic mobility loss in subjects with moderate to very severe COPD May improve after In-Patient pulmonary rehabilitation. Respir Care. 2018;63:1271–80.
31. De Groote A, Wantier M, Cheron G, Estenne M, Paiva M. Chest wall motion during tidal breathing. J Appl Physiol (1985). 1997;83:1531–7.
32. Cohen E, Mier A, Heywood P, Murphy K, Boultbee J, Guz A. Excursion-volume relation of the right hemidiaphragm measured by ultrasonography and respiratory airflow measurements. Thorax. 1994;49:885–9.
33. Houston JG, Angus RM, Cowan MD, McMillan NC, Thomson NC. Ultrasound assessment of normal hemidiaphragmatic movement: relation to inspiratory volume. Thorax. 1994;49:500–3.
34. Plathow C, Ley S, Fink C, Puderbach M, Heilmann M, Zuna I, Kauczor HU. Evaluation of chest motion and volumetry during the breathing cycle by dynamic MRI in healthy subjects: comparison with pulmonary function tests. Invest Radiol. 2004;39:202–9.
35. Tanimoto D, Ito K, Higashi H, Yamamoto A, Kanki A, Yasokawa K, Tamada T. Kinematic magnetic resonance imaging of the thorax using 2-Dimensional balanced subsecond Steady-state free precession sequence during forced breathing in comparison with spirometry. J Thorac Imaging. 2018;33:184–90.
36. Rocha FR, Brüggemann AK, Francisco DS, Medeiros CS, Rosal D, Paulin E. Diaphragmatic mobility: relationship with lung function, respiratory muscle strength, dyspnea, and physical activity in daily life in patients with COPD. J Bras Pneumol. 2017;43:32–7.
37. Gibson GJ. Diaphragmatic paresis: pathophysiology, clinical features, and investigation. Thorax. 1989;44:960–70.

Publisher's note